Interactions between structural and chemical biomimetism in synthetic stem cell niches

Michele M Nava[1], Manuela T Raimondi[1], Caterina Credi[1], Carmela De Marco[1], Stefano Turri[1], Giulio Cerullo[2] and Roberto Osellame[2]

[1] Department of Chemistry, Materials and Chemical Engineering 'Giulio Natta', Politecnico di Milano, 32, piazza Leonardo da Vinci, 20133, Milano, Italy

[2] Istituto di Fotonica e Nanotecnologie–CNR and Department of Physics–Politecnico di Milano, Piazza L. da Vinci 32, 20133 Milano, Italy

E-mail: michele.nava@polimi.it

RECEIVED
25 June 2014

REVISED
29 October 2014

ACCEPTED FOR PUBLICATION
2 December 2014

PUBLISHED
16 January 2015

1. Introduction

Stem cells (SCs) possess great potential for therapies in regenerative medicine to restore the function of injured cells, tissues and organs. However, before clinical applications, several difficulties in efficiently controlling and manipulating SC fate should be overcome. A promising strategy to achieve this goal consists in regulating stem cell function in artificial microenvironments, also called 'synthetic niches' (Joddar *et al* 2013). Synthetic niches, mimicking individual aspects of the interactions between stem cells and the extracellular surroundings, including biochemical (e.g. delivery of soluble factors) and/or biophysical factors (e.g. substrate stiffness), would yield several benefits in understanding cell behavior in truly three-dimensional (3D) conditions. For example, hydrogel-based synthetic niches composed of hyaluronic acid (Bian *et al* 2013) and gelatins (Angele *et al* 2009) were recently used to study the role of matrix microenvironment (architecture, composition, stiffness) in chondrogenic commitment of mesenchymal stromal cells (MSCs).

Within this context, an emergent tool to drive stem cell function is the employment of purely mechani-cal cues, such as patterned culture substrates inducing different levels of cell deformation. Alterations in the cell adhesion configuration are believed to affect cell cytoskeletal organization which in turn might promote or inhibit changes in the nuclear morphology, nuclear physical and mechanical properties, DNA packing and gene activation (Iyer *et al* 2012, Nava *et al* 2012).

However, self-assembled scaffolds (Angele *et al* 2009, Bian *et al* 2013) do not allow a fine control on the geometrical structure. A novel technology to fab-ricate advanced culture substrates, which overcomes this limitation, is two-photon laser polymerization (2PP) (Maruo *et al* 2008). This laser rapid prototyping

technique allows for the fabrication of 3D arbitrary microarchitectures, with a spatial resolution of the order of 100 nm, a value below the light diffraction limit. Therefore, it is the only technique able to fabricate 3D artificial niches with finely regulated geometries at the cell scale (10 μm). Photopolymerization occurs by nonlinear two-photon absorption induced by femtosecond laser pulses in transparent materials that are basically hybrid inorganic-organic resins (Ovsianikov *et al* 2012). The biocompatibility of these materials has been extensively demonstrated (Raimondi *et al* 2012, Danilevičius *et al* 2013). The complexity and high-level of control of the geometry of these 3D micro–scaffolds requires the use of materials with high mechanical stiffness. This does not allow tailoring this parameter arbitrarily.

In this work, we have developed a strategy to achieve the independent control of both the 3D geometry, allowed by 2PP, and substrate stiffness. This result is obtained by coating the above-mentioned artificial niche substrates using thin layers of hyaluronan-based and gelatin-based hydrogels, with tailored mechanical and physico-chemical properties. We used this culture model to study the interactions between structural and chemical biomimetism on the response of MSCs in terms of proliferation and differentiation. To this purpose, we firstly verified the biocompatibility of the coated synthetic niche substrates using an immortalized cell line. Then, we cultured MSCs on the substrates and we evaluated their morphology, proliferation and differentiation.

2. Materials and methods

2.1. Fabrication of the synthetic niche substrate by two-photon laser polymerization (2PP)

The niche geometry was selected from eight previously tested ones, as the one most favoring spontaneous MSC homing and proliferation (Raimondi *et al* 2013). Individual niches (figure 1(*a*)) were 30 μm high and $90 \times 90\,\mu m^2$ in transverse dimensions and consisted of a lattice of interconnected lines, with a graded spacing between 10 and 30 microns in the transverse direction and with a uniform spacing of 15 μm in the vertical direction. The 3D niche was surrounded by 4 outer confinement walls formed by horizontal rods spaced by 7.5 μm resulting in small gaps of 2 μm, which enable nutrients to pass through to the cells in the niche but prevent cells which have migrated to the niche from escaping through the sides. All the structural truss elements had an elliptical cross section with major axis of 5 μm and minor axis of 2.5 μm. These dimensions could be significantly reduced by fully exploiting the 2PP technique potential, however they are required to provide mechanical stability to the engineered niches.

The niches were laser written directly onto circular coverslip glasses of 150 μm thickness and 12 mm diameter (BioOptika). On each coverglass, three niches were arranged in a triangular pattern, at a relative distance of 200 μm (figure 1(*b*)). To improve the adhesion of the scaffolds to the substrate, a silanization process was performed on the coverslip glasses before depositing the photoresist.

In this work, we fabricated the niches in an organic-inorganic photoresist (SZ2080 in the following) with 1% concentration of Irg photoinitiator (Irgacure 369, 2-Benzyl-2-dimethylamino-1-(4-morpholinophenyl)-butanone-1) (Raimondi *et al* 2014). In our previous work (Raimondi *et al* 2013) we formed the niches in the same SZ2080 photoresist but with Bis photoinitiator (Michler's ketone, 4,4′-bis(dimethylamino)benzophenone) which showed strong autofluorescence, hindering the characterization of the fluorescent markers for cell proliferation. To achieve an efficient two-photon absorption process in the Irg-based SZ2080, we employed an Yb-based amplified laser (femtoREGEN, High Q Laser), producing 400 fs pulses at 1040 nm wavelength and 1 MHz repetition rate. The pulses were focused with a 1.4-NA oil immersion microscope objective (Plan-APOCHROMAT, 100 ×, Zeiss). Careful optimization of laser writing conditions allowed us to identify an attractive processing window with 0.7 mm s^{-1} writing speed and 23 mW average power. Computer-controlled, 3-axis motion stages (ABL-1000, Aerotech) were used to translate the sample relative to the laser to form the desired 3D microarchitecture of the niches. To improve the robustness of the structures a double irradiation scan was performed with a lateral shift of 500 nm between the two scans.

2.2. Design of the hydrogel coatings

Hyaluronic acid (HA) and gelatin hydrogels were prepared exploiting both chemical and photochemical crosslinking methods. Products and reagents, apart when not specified, were all purchased from Sigma-Aldrich and used without any purification.

2.2.1. Hyaluronic acid–divinyl sulfone (HA–DVS) chemical hydrogels

Powdered Hyaluronic acid sodium salt (NaHA, 1.6×10^6 g mol^{-1}), obtained by fermentation of *Streptococcus equi* bacteria, was dissolved in alkaline solution (0.5% w/v, 0.2 M NaOH, pH 13) and divinyl sulfone (DVS) was added as crosslinking agent directly into the HA solution (Balazs and Leshchiner 1986, Collins and Birkinshaw 2011) with HA : DVS molar ratio 1 : 10 (respect to HA primary hydroxyls). After stirring the mixture for 4 min in a closed vial to allow DVS uniform diffusion without its uncontrolled evaporation, the reaction was allowed to proceed for 12 h at 4 °C.

2.2.2. Synthesis of glycidyl methacrylated-hyaluronic acid (GMHA) hydrogels

Photocrosslinkable hydrogels were synthesized functionalizing HA chains with methacrylate groups. HA solution (1% w/v in DW) was reacted at room temperature for 24 h with a 20-fold molar excess of glycidyl methacrylate in the presence of 20-fold molar

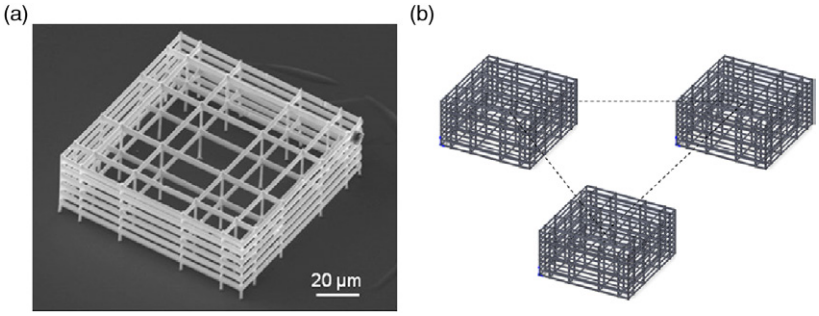

Figure 1. Geometrical configuration of the artificial niche substrate, which was laser-fabricated on glass coverslips by two-photon laser polymerization (2PP) into the SZ2080 photoresist using the Irgacure photoinitiator. (*a*) SEM of an individual 2PP niche, optimized for cell penetration in the larger central pores and optimized for a higher surface-to-volume for cell adhesion near the lateral vertexes. (*b*) On each coverglass, 3 niches were arranged in a triangular pattern. Their relative distance was set at 200 μm.

excess of triethylamine acting as a catalyst (Bencherif *et al* 2008, Prata *et al* 2010). Then the solution was precipitated twice in acetone, dissolved in DW, lyophilized (VirTis BenchTop Freeze dryer 2 K) and finally stored desiccated in the dark at −20 °C. H-NMR spectroscopy analyses were done on GMHA conjugates dissolved in D_2O in order to verify the efficiency of methacrylic functionalization (Baier Leach *et al* 2003). GMHA hydrogels were then crosslinked by expos-ing GMHA solution (0.2% w/v in phosphate buffered saline, PBS) to UV-light ($\lambda = 365$ nm, 4 mW cm^{-2}, 10 min exposure) in nitrogen atmosphere in the pres-ence of the photoinitiator Irgacure I2959 (1.5% w/v; Ciba Specialty Chemicals) and N-vinyl pyrrolidone (VP; 1.5% v/v), as reactive co-monomer as well as sol-vent for the photoinitiator.

2.2.3. Thiolated-gelatin (GEL-SH) chemically crosslinked hydrogels
Thiol-modified gelatin (carboxymethyl gelatin-thiopropanoyl hydrazide GTN-DTPH, Gelin-S™, Glycosan BioSystems, Inc.) was crosslinked exploiting a disulfide strategy using thiol-reactive crosslinker poly(ethylene glycol) diacrylate (PEGDA $M_w = 3.400$ g mol^{-1}, Extralink™, Glycosan BioSystems, Inc.) (Shu *et al* 2003). PEGDA solution (0.5% w/v in DW) was added into the thiolated macromonomer solution (0.25% w/v in DW) to have a thiol: C=C double bonds ratio ≈ 2 : 1 (Shu *et al* 2006). The mixture was stirred for 30 s and poured in a petri dish where the reaction was allowed to proceed overnight. Hydrogels mechanical properties can be tuned varying the concentration of both the thiolated gelatin and PEGDA solutions (Vanderhooft *et al* 2009).

2.3. Microfluidic coating of the synthetic niches
Different interactions at the interface between SZ2080 surfaces and the hydrogels were investigated to graft HA, GMHA and Gel-SH hydrogels in order to functionalize the 2PP-patterned samples. To overcome pore occlusion due to the viscosity and surface tension of the hydrogels solutions, together with the small pores dimensions, functionalization processes were scaled-down and performed in a microfluidic system assembled by reversibly sealing the glass substrate where the structures are laser written, with polydimethylsiloxane (PDMS) μ-channels (500 μm height, 200 μm width) after air-plasma surfaces activation (60 W, 60s PECVD System, Kenosistech).

2.3.1. Microchannel fabrication
PDMS liquid precursor and its curing agent (Sylgard® 184, Dow Corning) were mixed at 10 : 1 w/w and then the PDMS mixture poured onto an SU-8 (SU-8 2050, MicroChem, USA) mold on a silicon wafer fabricated according to the manufacturer instructions and silanized with 1H,1H,2H,2H-perfluorooctyltriethoxysilane (ABCR, Germany) to prevent PDMS adhesion on the SU-8 structures. The mixture was thermally crosslinked at 90 °C for 1 h.

2.3.2. Process used to coat the 2PP niches
HA : DVS hydrogels were immobilized on the niches through hydrogen bonding formation between the hydrophilic moieties of HA (–COOH or –OH) with hydrophilic groups generated on the photoresist surfaces after the air-plasma treatment (Suh *et al* 2005). HA : DVS mixture was pumped (Syringe Pump 11 Plus, Harvard Apparatus) at 3 μl min^{-1} for 2 h through the air-plasma treated niches. Then, the PDMS channels were peeled off and the reaction was allowed to proceed overnight at 4 °C.

The GMHA hydrogels were UV-photografted on the SZ2080 surfaces exploiting the free radical polymerization of the methacrylate groups of the GMHA with both the residual SZ2080 unreacted double bonds and the methacrylate groups generated on the SZ2080 sur-faces through a vapor phase silanization with 3-acry-loxypropyl methyldimethoxysilane (APMES, 12 h at 35 °C). GMHA solution (0.2% w/v in PBS) was fluxed at 3 μl min^{-1} through the scaffolds for 30 min. Then the PDMS was peeled off and the niches where UV-irradiated ($\lambda = 365$ nm, 4 mW cm^{-2}, 10 min exposure) in nitrogen atmosphere.

Finally, Gel-SH hydrogels were grafted using as intermediate linker the adhesive protein dopamine that can self-polymerize at alkaline pH to form polydopa-mine (PD) surface-adherent layer (Waite and Tanzer 1981, Lee *et al* 2007). A dopamine hydrochloride solu-tion (2 mg ml^{-1} in tris-HCl 10mM, pH 8.5) was first fluxed at 3 μl min^{-1} for 12 h. PDMS channels were then detached and PD-coated substrates were incubated overnight with 200 μl of Gel-SH : PEGDA solution in nitrogen atmosphere so that thiol groups of gelatin can be covalently conjugated to the PD layer via the quinone group (Lee *et al* 2009). At the end of all the processes the samples were washed with distilled water to remove material in excess.

Hydrogel coating efficiency was evaluated through environmental scanning electron microscopy (ESEM) analyses performed with an EVO 50 Extended Pressure microscope (Carl Zeiss).

2.4. Mechanical characterization of the niche coatings by swelling measurements and Flory–Rehner calculations

Swelling experiments following the Flory–Rehner theory (Flory 1953) were conducted to estimate the degree of hydrogels swelling which is strictly correlated to the crosslinked network density and to their mechanical strength (Anseth *et al* 1996, Credi *et al* 2014). The extent of swelling q_M was calculated by dividing the equilibrium-swollen gel mass (W_s) by the dried gel mass (W_d), both measured through thermogravimetric analysis (TGA, Q500, TA Instrument. Particularly, few milligrams of hydrogel (W_s) were collected from the functionalized niche surfaces, placed in the TGA weighing pan and slowly heated at 50 °C fixed-temperature until a constant mass (W_d) was achieved. The crosslink density $\upsilon = \rho_p / M_c$ was then determined by applying an expression of the Flory–Rehner equation, approximated for networks with low degrees of crosslinking swollen in good solvent:

$$q_e^{5/3} \cong \frac{M_c}{\rho_p V_1}\left(\frac{1}{2} - \chi\right),$$

where M_c is the average between crosslinks, V_1 is the molar volume of the solvent (18 $cm^3\,mol^{-1}$ for water), ρ_p is the density of the dry polymer (1.229 $g\,cm^{-3}$), χ is the Flory polymer–solvent interaction parameter estimated to be 0.473 (Baier Leach *et al* 2003) and q_e is the volumetric swelling ratio determined from q_M (Marsano *et al* 2000):

$$q_e = 1 + \frac{\rho_p}{\rho_s}(q_M - 1)$$

being ρ_s the density of the water.

Finally, through the rubber elasticity theory (Treloar 1975) the hydrogels Young's modulus E was estimated assuming a 0.5 Poisson's ratio (Hachet *et al* 2012):

$$E = 2\,G(1 + \nu),$$

where G is the shear modulus calculated fitting with Flory–Rehner crosslink density υ data the following relationship:

$$\upsilon = \frac{G}{RT}$$

being R the gas constant (8.314 $J\,mol^{-1}K^{-1}$) and T the temperature at which the modulus was measured (310.15 K).

2.5. Cell culture on the hydrogel-coated 2PP niche substrates and analyses

The study was conducted in two steps: first, we evaluated general aspects of biocompatibility of the hydrogel-coated 2PP niche substrates using immortalized cells and then we investigated the behavior of primary MSC. Unless otherwise specified, chemicals and chemofluorescent markers were purchased from Sigma-Aldrich; immunofluorescence markers from Thermo Scientific; cell culture media and plastics from Euroclone.

2.5.1. Immortalized cells

We used the MG63 human osteosarcoma cell line (86051601-1VL, Sigma-Aldrich) to assess aspects of biocompatibility of the niche substrates, including cell viability/cytotoxicity, cell adhesion and morphological compatibility. Cells were resuscitated and expanded in minimum essential medium (MEM) supplemented with 2mM glutamine, 10% fetal calf serum (FCS), 1% non-essential amino acids (NEAAs), and 1% penicillin/streptomycin, under 5% CO_2 atmosphere at 37 °C. Immortalized cells were cultured in standard flask until semi-confluence.

2.5.2. Mesenchymal stem cells

We used primary rat MSCs to study cell viability, adhesion, migration, proliferation and differentiation on the hydrogel-coated 2PP niche substrates. Briefly, bone marrow was obtained from 2 month-old Lewis or Sprague-Dawley rats. Rats were sacrificed and femurs and tibias were aseptically removed. Bone marrow was flushed from the shaft of the bones with a-MEM medium (Invitrogen-Gibco) containing 5% FCS plus 1% penicillin/streptomycin and then filtered through a 100 μm sterile filter to produce a single-cell suspension. MSCs were recovered from bone marrow by their tendency to adhere tightly to plastic culture dishes. Filtered bone marrow cells were plated in α-MEM supplemented with 20% FCS and 1% penicillin/streptomycin and allowed to adhere for 24 h. Non-adherent cells were then removed. The medium was changed regularly every 3 d until confluence. Adherent cells were detached by trypsin-EDTA (0.5 to 0.2 g $m1^{-1}$; Invitrogen), counted and cryo-preserved in α-MEM supplemented with 30% FCS and 5% dimethyl sulfoxide (DMSO) until use. After resuscitation, cells were plated and cultured until semi-confluence in standard flasks in complete medium. The animal protocols used in this

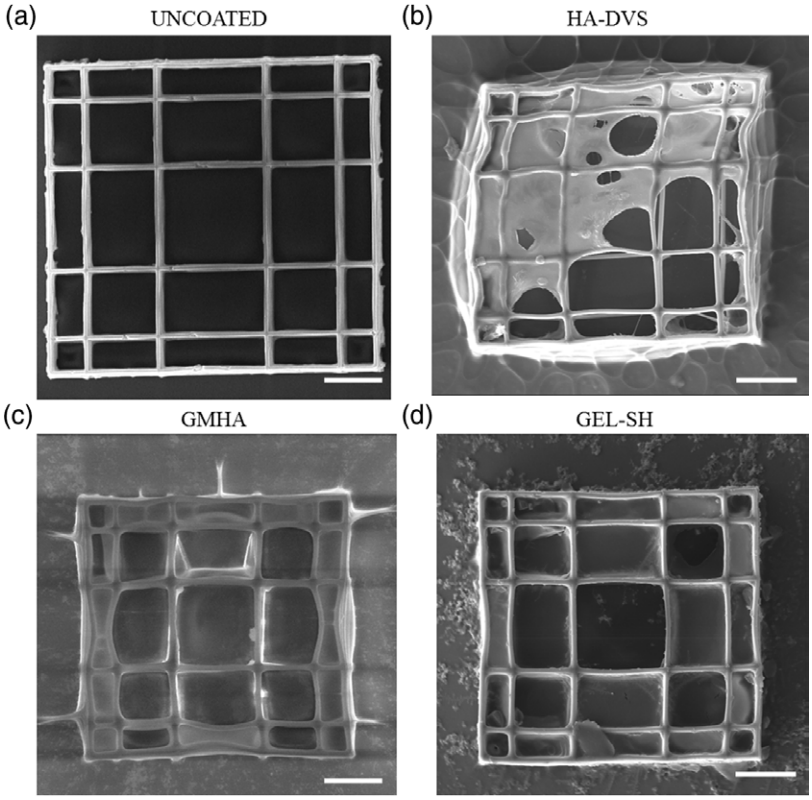

Figure 2. SEM images of the 2PP niche substrates shown in vertical projection. (*a*) Uncoated niche, (*b*) niche coated with a hyaluronic acid–divinyl sulfone (HA–DVS) hydrogel, (*c*) niche coated with a glycidyl methacrylated-hyaluronic acid (GMHA) hydrogel and (*d*) niche coated with a thiolated-gelatin (GEL-SH) hydrogel. Scale bar is 20 μm.

study comply with the institutional protocols for ethical use currently in force.

2.5.3. Substrate preparation and cell seeding

For cell seeding, cells were trypsinized and counted. The hydrogel-coated 2PP niche substrates (hereon called 'samples') were washed thoroughly, kept for 12 h in deionized water, disinfected for 12 h in 70% ethanol, washed repeatedly in sterile deionized water, dried and UV-sterilized. Each sample was positioned in a well of ultra-low attachment 24 multi-well plates (Costar 3473, Corning). MG63 cells and MSCs were suspended in their proper complete culture medium and seeded on the samples directly in the wells, at a density of 20 000 cells cm^{-2}. MG63 cells were incubated for 3 d, while MSCs for 14 d, with medium freshly replaced every day.

2.5.4. Morphological examination

The live cellularized samples were imaged in their wells in phase contrast every day using an inverted phase contrast/fluorescence microscope (IX70, Olympus) equipped with a cooled high-resolution color video camera (4083.CL3, Optika).

For SEM, the cellularized samples were fixed in the wells in 1.5% glutaraldheide and 0.1M sodium cacodylate and dehydrated in a graded series of ethanol. The samples were extracted from the wells, air dried, glued onto SEM stubs and gold-coated in a vacuum ion coater. All observations were carried out at 17.5 kV using an EVO 50 Extended Pressure system (Carl Zeiss).

2.5.5. Biochemical assays

Cell viability was assessed by two colorimetric methods: the ethidium/calcein assay to assess membrane integrity and a mitochondrial dye inclusion (3-(4,5-dimethylthiazol-2-yl)-2,5-diphenyltetrazolium bromide, MTT, Sigma Chemical) assay to assess metabolic activity.

The cellularized samples were marked in the wells using a live/dead viability/cytotoxicity kit (L3224, Invitrogen-Molecular Probes), in which the polyanionic dye calcein is retained within live cells producing green fluorescence, and ethidium homodimer-1 (EthD-1) enters cells with damaged membranes and binds to nucleic acids, producing a red fluorescence. The samples were incubated in 2μM calcein and 4μM EthD-1 solutions for 45 min and imaged directly in the wells.

The cell metabolic activity was assayed using the MTT assay. The dye was converted in insoluble formazan crystals by the cells and subsequently solubilized in DMSO. Absorbance of the converted dye was determined 570–630 nm with a spectrophotometer (Infinite Pro 200, Tecan).

The DNA content was assessed on the cell lysate. The culture medium was replaced with deionized water and the culture plate containing the cellularized samples was frozen at −80 °C and incubated at 37 °C repeatedly.

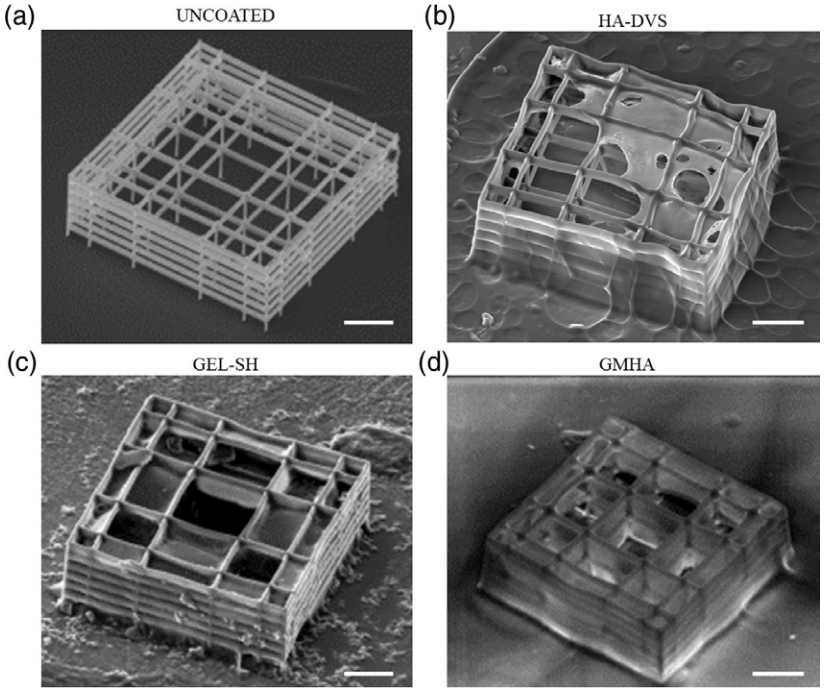

Figure 3. SEM images of the 2PP niche substrates shown in 45°-tilted projection. (*a*) Uncoated niche, (*b*) niche coated with a Hyaluronic acid–divinyl sulfone (HA–DVS) hydrogel, (*c*) niche coated with a glycidyl methacrylated-hyaluronic acid (GMHA) hydrogel and (*d*) niche coated with a thiolated-gelatin (GEL-SH) hydrogel. Scale bar is 20 μm.

The DNA absorbance was measured at 260 nm directly on the cell lysate with a spectrophotometer (Infinite Pro 200, Tecan) equipped with a NanoQuant Plate.

2.5.6. Fluorescence staining and confocal microscopy
For confocal microscopy, the cellularized samples were fixed in the wells in paraformaldehyde 2%, permeabilized with Triton 0.2%, blocked with 3% bovine serum albumin (BSA) plus 10% FCS to avoid unspecific labeling, and fluorescently marked. DNA was stained by incubation with 4′,6′-diamidino-2-phenylindole dihydrochloride (DAPI) in solution at 10 µg ml^{-1}. Cell proliferation was studied by detection of the Ki67 antigen, which is expressed by cells in all the phases of the division cycle, using a red Cy3-conjugated mouse anti-Ki67 monoclonal antibody (NCL-Ki67-MM1, Novocastra). Collagen type I, collagen type II and Osteocalcin were immunolabeled with primary antibodies and then marked in red using Cy3-conjugated secondary antibodies. MG63 cells expressing all the investigated markers (Pautke *et al* 2004) were used as positive controls for all the immunostaining procedures. Image acquisition and 3D reconstruction were performed at 15× and at 63× with a laser confocal microscope (LSM 510 Meta, Carl Zeiss).

2.5.7. Statistical analysis
Cell count was performed on images acquired in fluorescence on the green/red-labeled samples and DAPI-labeled samples, in transmission by an inverted microscope. By this method, all the cell nuclei present on the sample were visualized in projection on the images, instead of what happens in confocal acquisitions where only the projection of a limited sample volume above the cell-populated coated glass surface is visualized. MG63 cell viability was assessed visually by counting viable (green) and non-viable (red) cells in square regions of 100 × 100 μm^2. MSC cell count was assessed visually on the DAPI-marked cells, by counting the cell nuclei in square regions of 100 × 100 μm^2. In both cases, cell density was obtained by dividing the cell count of each region by the area of the square region. Results of the cell counts were assigned to experimental groups based on the coating type. For each coating type, cell counts were assigned based on the count location: (i) coated glass (flat), (ii) coated niche internal volume (niche).

Table 1. Young's moduli experimentally estimated for the three hydrogels used to coat the artificial niche substrates.

	Young's modulus (kPa)
HA–DVS	∼20
GMHA	∼0.4
GEL-SH	∼0.2

For collagen I-positive cells quantification, DAPI-labeled (blue) and TRITC-labeled (red) fluorescence pictures were converted to grayscale, filtered and manually thresholded. To avoid an overestimation of the fluorescent signal, niches were subtracted before converting into binary format. Then, the overall nuclei area and collagen area were measured on the resulting binary pictures ($n = 3$ pictures for each sample). Cells positive to collagen-I, grouped according to the

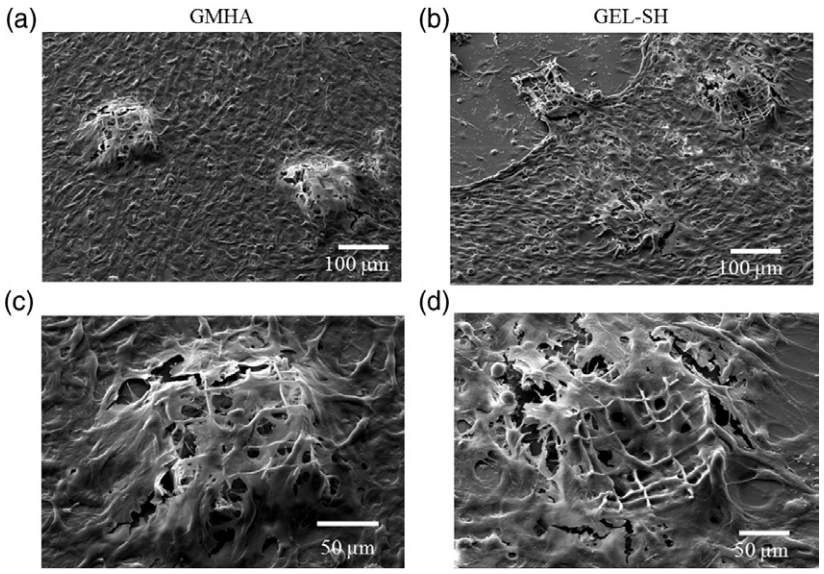

Figure 4. Results of the biocompatibility tests for the MG63 cells cultured on the coated niche substrates at 3d. SEM images of a (*a*),(*c*) GMHA-coated and a (*b*),(*d*) GEL-SH-coated cellularized niche substrate. After three days of culture, MG63 cells proliferated until confluence on the flat coated-surface surrounding the niches, migrated in the niches by climbing their external walls, and aggressively invaded the internal niche volumes.

above-mentioned count location, were calculated as the percentage ratio between the collagen area and the nuclei area. The groups were compared using one-way analysis of variance (ANOVA) for independent samples. Pair-wise comparisons among groups were determined with the Tukey HSD test, or with the Student t-test for independent samples. Differences were considered to be significant if $p < 0.05$.

3. Results

3.1. Coating efficiency

ESEM analyses were performed on the hydrogel-coated 2PP niche substrates to evaluate the coating processes efficiency. Exploiting the microfluidic system, the hydrogel solutions were forced to penetrate within the synthetic niches at an experimental flow rate necessary to uniformly fill the microporous structures removing unreacted material but avoiding samples collapse due to high shear stresses. Homogeneous coating of the external walls was achieved as attested by the presence of a thin hydrogel layer on the microstructures if compared to uncoated samples (figures 2(*a*)–(*d*)). Even the internal niches volumes were functionalized almost without affecting the overall microporosity (figures 3(*a*)–(*d*)). However, HA : DVS hydrogels grafting, which exploits physical interactions at the interface of the two materials, could lead to non-specific adsorption resulting inefficient due to an excess of material deposition (figure 2(*b*)). Moreover, a stronger bonding based on covalent interactions between hydrogels and photoresist, as for GMHA and Gel-SH, should be more suited to avoid the coating detachment which could be caused both by compressive forces that cells induce while adhering on the substrates and by the dynamical swelling behavior of hydrophilic polysaccharides (Mathe *et al* 1999). The coating process is not specific to the microscaffolds, but also covers the surrounding glass surface; indeed, it is technologically very challenging to confine the coating to the size of the microstructures ($90 \times 90 \times 30$ μm^3). Therefore, each coated 2PP sample shows a coated glass region (flat) and coated niches (niche).

3.2. Mechanical properties of the coatings

The mechanical characteristics of the hydrogel coated samples were indirectly evaluated measuring the extent of hydrogels swelling q_M through TGA analyses implemented on few milligrams of hydrogels sampled from the functionalized 2PP surfaces. TGA data were then used to fit an approximate expression of the Flory–Rehner equation in order to calculate hydrogels crosslink density, which is related to the elastic modulus through the rubber elasticity theory. Flory–Rehner calculations lead to elastic modulus values for hydrogels synthesized (table 1) encompassing the range of physiological niches values (Engler *et al* 2006) and varying from 20 kPa for HA : DVS samples to 0.2 kPa for Gel-SH samples Particularly, HA : DVS hydrogels stiffness was obtained keeping control over crosslinking conditions such as DVS-content (10-fold molar excess respect to HA) and curing time (12 h) (Credi *et al* 2014). Irgacure content for GMHA and thiol: C=C double bonds ratio for Gel-SH samples were the key parameters to be considered in hydrogels mechanical properties tuning. Therefore, it was possible to study the effect that tuning scaffold stiffness and varying hydrogel chemistry could have on MSCs behavior.

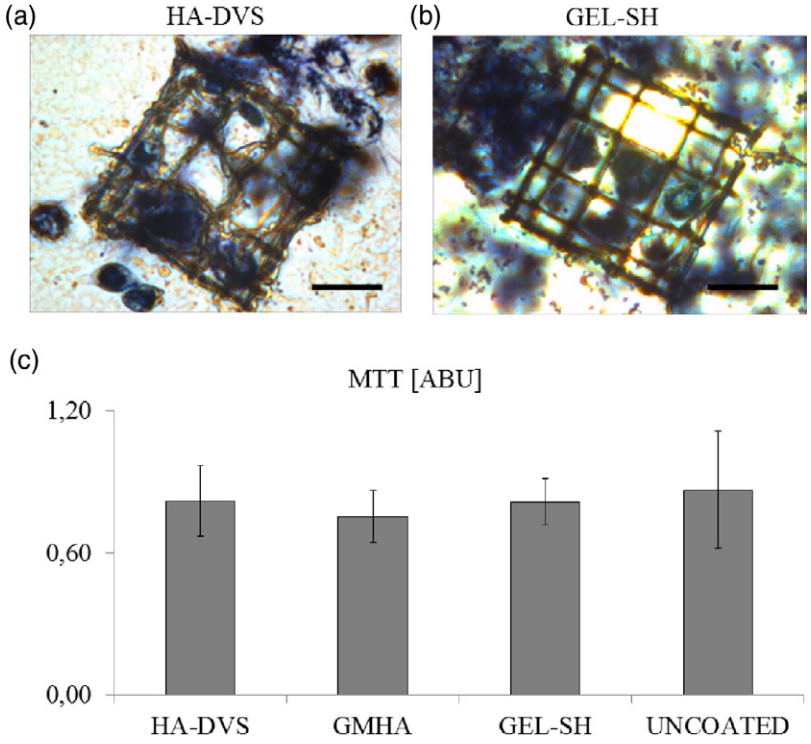

Figure 5. Results of the biocompatibility tests for the hydrogel-coated niche substrates after 3 d of culture of MG63 cells. Images of cells after MTT dye inclusion for (*a*) HA-DVS-coated and (*b*) GEL-SH coated cellularized niche. Images show that the mitochondrial dye (in purple) was incorporated by metabolically active cells in all areas of the niche substrate. (*c*) Absorbance of the MTT converted dye measured for cells cultured on the hydrogel-coated niche substrates and cells cultured on control (uncoated) substrates. Scale bar is 50 μm.

3.3. Biocompatibility of the hydrogel-coated niche substrates

We used an immortalized cell line to evaluate aspects of biocompatibility, i.e. cell adhesion to the coated 2PP samples, their morphological compatibility, cell metabolic activity and cell viability. Optimal cell adhesion was observed for all the coated samples. The MG63 cells in three days proliferated to confluence homogeneously on the flat coated-surface surrounding the niches and invaded the internal niche volumes by climbing the external confinement grids (figures 4(*a*)–(*d*)). To evaluate the cell metabolic activity when cultured on the niche substrates, we performed an MTT assay. Acquired images in bright field of a cellularized HA–DVS-coated niche (figure 5(*a*)) and a GEL-SH-coated niche (figure 5(*b*)) show an intense purple color both for cells adherent to the glass surface and for cells anchored to the internal surface covered with a thin layer of HA–DVS and GEL-SH hydrogels, respectively. Absorbance of the converted dye measured for the coated coated 2PP samples and for the uncoated glasses (uncoated controls) is illustrated in figure 5(*c*). We observed that the metabolic activity of MG63 cells cultured in samples with different coatings and on uncoated controls does not show any statistically significant difference.

Cell viability was assessed by performing a Live/Dead assay. Phase contrast images and the corresponding merged fluorescence images are summarized in figure 6. With the exception of HA–DVS-coated substrates, immortalized cells proliferated rapidly on the coated-glass surface forming a rather homogeneous monolayer and also colonized the niches (figures 6(*a*)–(*c*)). We observed that most cells on the coated-glass surface were viable in all samples (figures 6(*d*)–(*e*)). Nonviable cells (stained in red) were absent within the internal volume of the niches, while a few dead cells could be seen on the external niche walls when coated with GMHA (figure 6(*e*)) and GEL-SH (figure 6(*f*)). We quantified visually the number of viable cells in each coated sample. The diagram in Figure 6(*g*) illustrate the percentage of viable cells normalized to the total number of cell counted in a reference area ($100 \times 100\,\mu m^2$). Cells were grouped according to the location into the samples. While all cells in the coated niches are viable (viable cells is equal to 100%), the percentage of viable cells anchored on the niche external walls are 94.73 ± 4.12%, 84.20 ± 7.14% and 89.47 ± 10.20% in HA–DVS-, GMHA- and GEL-SH-coated substrates, respectively. Viable cells on coated-flat surfaces are 90.16 ± 4.08%, 92.31 ± 5.45%, and 86.08 ± 5.09% in HA–DVS-, GMHA- and GEL-SH-coated substrates, respectively.

3.4. Results of MSC culture on the hydrogel-coated niche substrates

We used primary rat MSCs to study cell morphology, metabolic activity, proliferation and differentiation

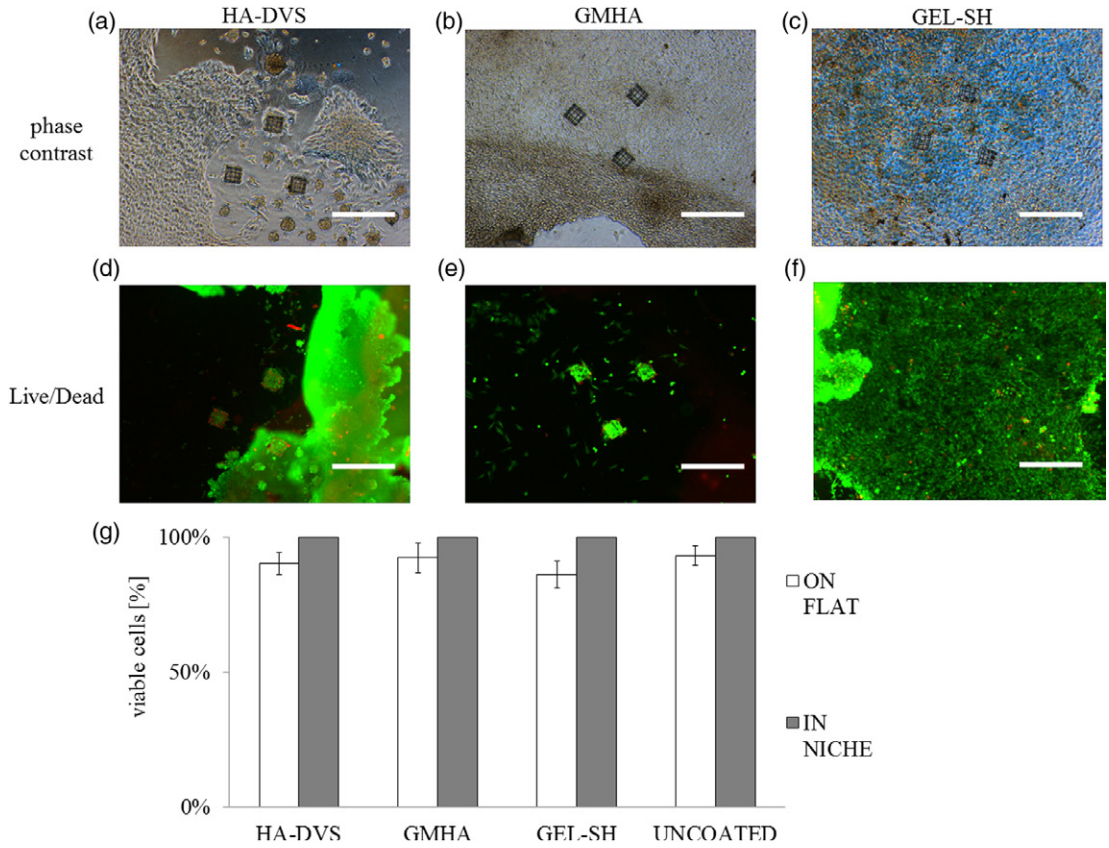

Figure 6. Results of the biocompatibility tests for the hydrogel-coated niche substrates after 3d of culture of MG63 cells. Phase contrast of cellularized (*a*) HA–DVS-coated substrates, (*b*) GMHA-coated substrates and (*c*) GEL-SH-coated substrates. Fluorescence Live-Dead images of cellularized (*d*) HA–DVS-coated substrates, (*e*) GMHA-coated substrates and (*f*) GEL-SH-coated substrates (viable cells in green and dead cells stain red). (*g*) Diagram illustrating the percentage of viable cells normalized to the total number of cell counted in a reference area (100×100) μm^2 grouped according to the location in the substrates. Scale bar is 200 μm.

when cultured on the niche substrates. Extensive cell adhesion to the niches was observed (figures 7(*a*)–(*f*)). Cells adhered and proliferated on the coated-glass surface and migrated toward the coated-niches from the surrounding monolayer, invaded the niches by climbing the external confinement walls and adhered to the internal niche lattice. After two weeks of culture, cells formed aggregates within the 3D niche microstructure. For example, in HA–DVS-coated substrates cell aggregates formed on the top of the coated niche (indicated by the arrow in figure 7(*a*)). In GMHA-coated substrates, cells established small aggregates within the niches (figures 7(*b*) and (*e*). Conversely, few cells were observed on the GEL-SH coated niches both on the flat coated-surface and in the internal niche volume where cells assumed a flat and elongated spindle-like shape (figures 7(*c*) and (*f*)).

We estimated the cell density after 14 culture days both for cells located on the coated surface (flat) surrounding the niches, and for the cells inside the coated niches (niche internal volume). Cell density was measured visually on the DAPI-labeled pictures of cellularized niche substrates by counting cells over comparable areas of $100 \times 100\,\mu$m^2 (figures 8(a)–(*f*)). The calculated cell density in HA–DVS- and GMHA-coated flat surfaces were 7.89 ± 2.37 cells/($100 \times 100\,\mu$m^2) and 6.57 ± 2.98 cells/($100 \times 100\,\mu$m^2), respectively. These values are 1.65-fold and 1.37-fold significantly greater than the cell density estimated on cultured uncoated glass surfaces. The cell density estimated in GEL-SH-coated surfaces was 3.36 ± 2.16 cells/($100 \times 100\,\mu$m^2), 1.30-fold significantly lower than cultured uncoated glasses. The same trend was observed for the cell density estimated in the internal niche volume. The cell density in uncoated niches was 16.77 ± 2.91 cells/($100 \times 100\,\mu$m^2), greater than the ones estimated in HA–DVS-coated niches (13.99 ± 2.14 cells/($100 \times 100\,\mu$m^2)) and GMHA-coated niches (13.58 ± 1.91 cells cells/($100 \times 100\,\mu$m^2)). The cell density in GEL-SH-coated niches is 6.17 ± 2.37 cells/($100 \times 100\,\mu$m^2), the lowest among the samples tested. It is worth noting that the cell densities in coated niche substrates were significantly lower compared to the one assessed for uncoated niche substrates.

Cell differentiation showed quite different trends depending on the type of surface coating and on the cells location on the coated samples. As shown in figures 9(a) and (*b*) respectively, cells in HA–DVS- and GMHA-coated niches were systematically negative for collagen I and all the differentiation markers tested. Collagen I positive stained cells (red) are located on the

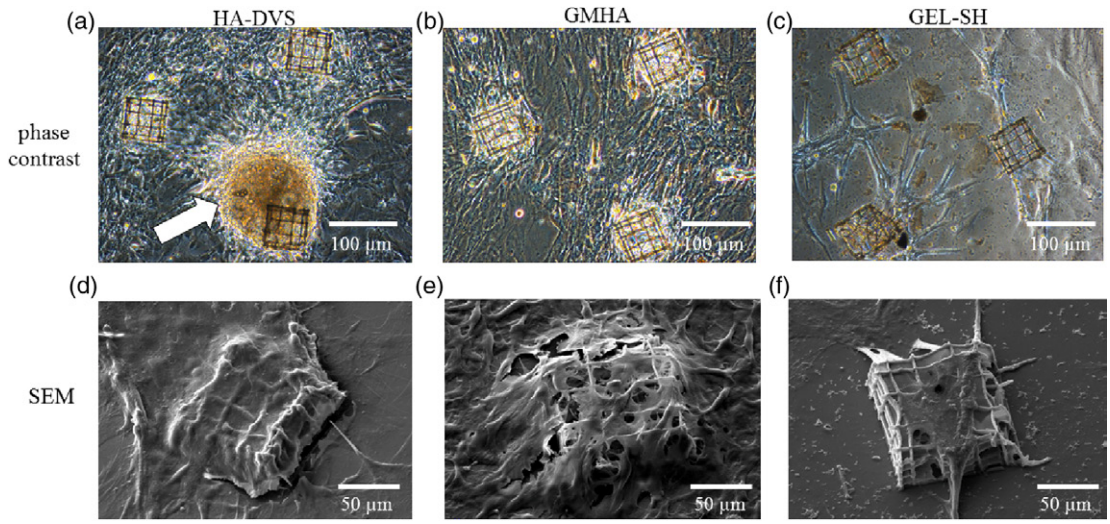

Figure 7. Results of MSC cells cultured on the coated niche substrates at 14d. Phase contrast pictures of (*a*) HA–DVS-coated substrate, (*b*) GMHA-coated substrate and (*c*) GEL-SH-coated substrate. The arrow in (*a*) indicates an aggregate that has formed on the top of a coated niche. SEM pictures of (*d*) HA–DVS coated niche, (*e*) GMHA-coated niche and (f) GEL-SH-coated niche.

coated flat surface surrounding the niches. Cells located far from the niches both on HA–DVS- and GMHA-coated flat surfaces (figures 9(c) and (*d*), respectively) stained positive to collagen I. Conversely, in the internal volume of the GEL-SH-coated niches we observed the expression of collagen type-I, an early marker of differentiation toward the osteo-chondral lineage (figures 10(a) and (*b*)).

We quantified collagen I positive cells normalized to the number of cells both on coated and uncoated samples. Cells on HA–DVS- and GMHA-coated flat substrate are 56.10 ± 12.50% and 38.08 ± 12.86% positive, percentages that are significantly greater than those observed for cells on flat GEL-SH-coated samples and on flat uncoated samples. Cells on GEL-SH-coated flat substrates are 16.62 ± 2.20% positive, significantly less than collagen I expression in uncoated flat surfaces. No positivity to collagen I was found in the HA–DVS- and GMHA-coated niches, as well as in uncoated niches. Cells in GEL-SH-coated niches show the greatest positivity to collagen I (37.24 ± 6.54% of positive cells), even though few cells are located in the niches and a few of them were anchored to the bottom coated flat surface of the substrate, as deduced by the well-spread morphology of the nuclei.

Finally, we evaluated the specific metabolic activity of cells cultured on the hydrogel-coated samples, calculated as the ratio between the MTT absorbance and the DNA content (figure 10(*d*)). Coherently with the results from immunofluorescence, the MTT–DNA ratio for GEL-SH-coated substrates was 39.7% greater than the ones measured for HA–DVS and GMHA samples, respectively, while it did not significantly differ from the value measured for uncoated flat samples, in which spontaneous differentiation toward the osteo-chondral lineage has been observed (Raimondi *et al* 2013, 2014).

4. Discussion

Increasing evidences have shown that mechanical cues (e.g. substrate stiffness, topography and 3D microarchitecture) are able to drive stem cell function *in vitro*. Indeed, cell-material interactions may induce changes in the adhesive configuration, which in turn may affect nuclear morphology, architecture and functions. In this work, we applied 2PP to fabricate a synthetic niche substrate for culturing MSC. 2PP is a rapid prototyping technique that allows fabricating 3D arbitrary microarchitectures with a spatial resolution of 100 nm. The versatility and the high resolution make 2PP the suitable technique to fabricate microscaffolds interacting at the cell scale. Here, we fabricated three niches arranged in a triangular pattern where the relative distance was set at 200 μm. The niche geometry was selected from eight previously tested ones, as the one most favoring spontaneous MSC homing and proliferation (Raimondi *et al* 2013). To ensure a high-level of control of the geometry of this 3D scaffolds the use of materials with high mechanical stiffness is required. Therefore, to modulate the material stiffness sensed by cells that anchor to the microscaffold, we coated these microstructures using hyaluronan-based and gelatin-based hydrogels, with tailored mechanical and physico-chemical properties aiming to study the synergistic effect of the microgeometry and the substrate stiffness on stem cell function.

From a technological perspective, we demonstrated the feasibility of the coating procedure. Indeed, hydrogel solutions homogeneously coated both the external walls and the internal niche volume without affecting the overall microporosity (figures 2 and 3). Due to technological reasons and to the overall size of the microstructures ($90 \times 90 \times 30\,\mu m^3$), the coating process is

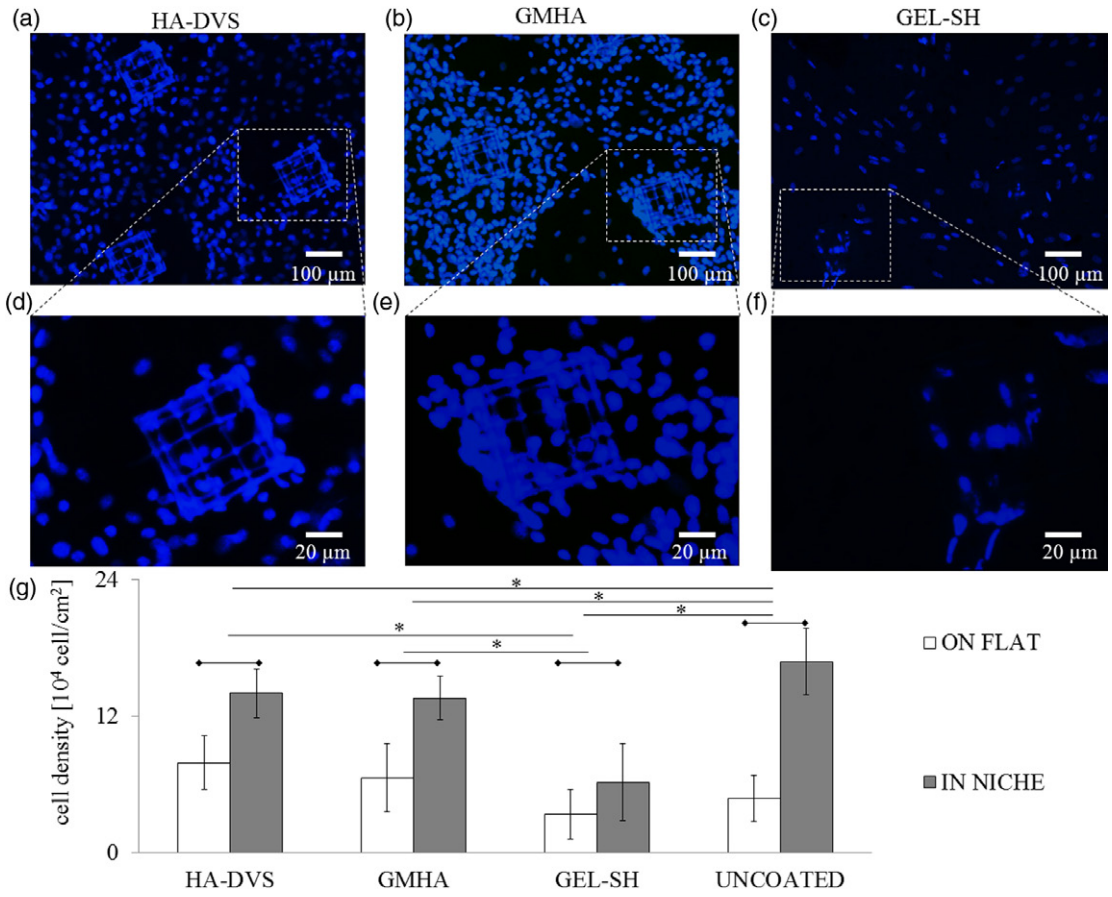

Figure 8. MSC cells cultured on the coated niche substrates at 14 d. DAPI-labeled pictures of the coated samples at low (*a*)–(*c*) magnification and (*d*)–(*f*) zoomed view of a single coated microstructure at higher magnification. Both MSC density on (*a*) HA–DVS- and (*b*) GMHA-coated flat surface and in (*d*) HA–DVS- and (*e*) GMHA-coated niches are visually higher than the MSC density on (*c*) GEL-SH-coated flat surface and (*f*) GEL-SH coated niche. (*g*) Histogram illustrating the cell density calculated at two distinct locations on the substrate: on flat surface (on flat) and in the niche interval volume (in niche). All measurements are given as mean and standard deviation of $n = 9$ measurements; $^{*}p < 0.01$ for all pair-wise comparisons.

not specific to the microstructures. The advantage arising from this non-selective coating consists in the fact that we could observe, on the same sample, cells adhering on the flat surface and in the internal niche volume, while sensing the same substrate stiffness in each location of the sample.

Cell culture of MG63 on coated 2PP substrates proved that the different coatings do not modify significantly cell adhesion and morphology (figure 4) as compared to the uncoated niches (Raimondi *et al* 2013). To evaluate the biocompatibility of the hydrogel coatings on 2PP niches, MTT tests were performed: as shown in figures 5(*a*) and (*b*), active metabolic cells were found within the niche volume, and the MTT collected data demonstrated no significant difference in mitochondrial activity between coated 2PP samples and uncoated samples. We also performed Live/dead assays (figures 6(*a*)–(*f*)) and counted viable cells according to the locations in the samples (figure 6(*g*)). All cells in the coated niches were viable, while viable cells on niche external walls and on flat-coated substrates were both close to 90%. Following the positive results of MG63 cell viability, the coated 2PP scaffolds were tested on rat MSCs.

Compared to the experimental outcomes reported on uncoated 2PP substrates (Raimondi *et al* 2013, 2014), we observed that the different coatings had significant effects on several culture parameters (figures 8(*a*)–(*f*)). Firstly, the cell density calculated on the flat-coated substrates is 1.65-fold (HA–DVS coated flat surface) and 1.37-fold (GMHA-coated flat surface) greater than the cell density estimated in uncoated flat surfaces. Conversely, the cell density on the GEL-SH coated substrates is 1.30-fold lower than the one calculated for the uncoated flat substrates. Concerning the cells populating the coated niche volume, we observed that the homing effect, which was very strong in uncoated 2PP niches, was significantly reduced in the coated 2PP niches, particularly in GEL-SH coated niches, where the cell density measured was 2.70-fold lower than in uncoated niches (figure 8(*g*)). A possible explanation for these results may be that cells sense differently the stiffness of substrates that are closer to the physiological range (table 1) compared to non-physiological values (in uncoated samples). Basically, cells tended to adhere and proliferate more on flat surfaces with a relatively high stiffness (as in HA–DVS- and GMHA-coated

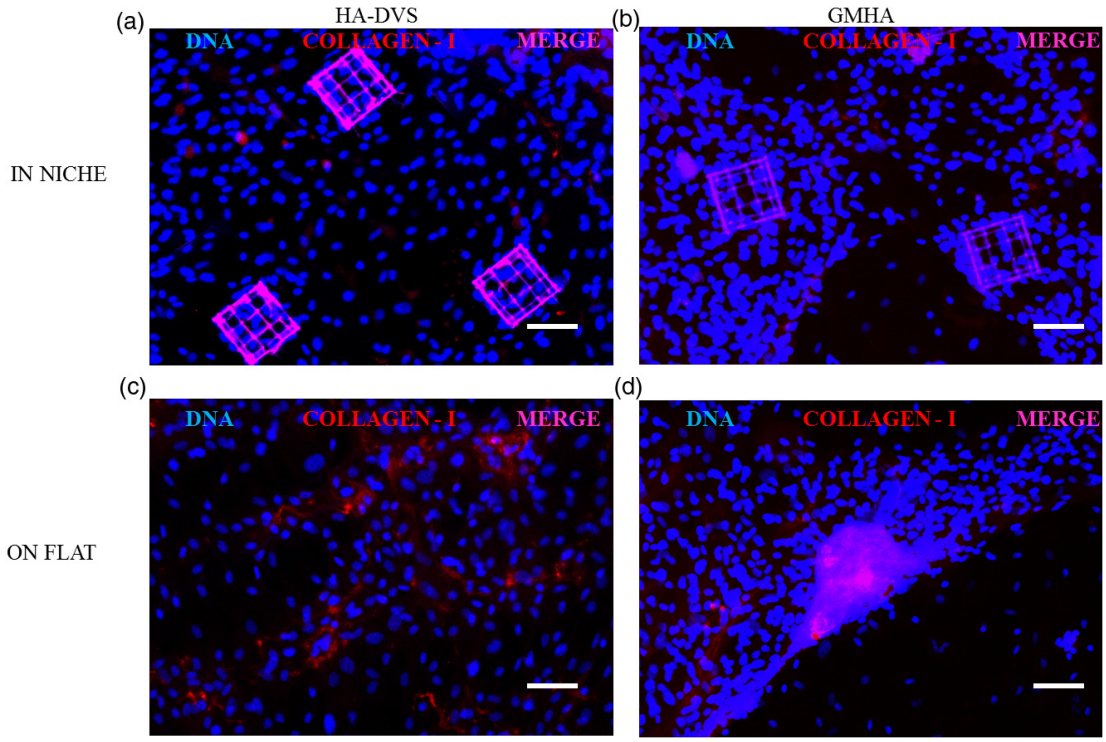

Figure 9. MSC cells cultured on the coated niche substrates at 14 d. Fluorescence images of HA–DVS- and GMHA-coated samples acquired on different locations of the coated samples. Cells in the internal niche volume stain negative for collagen I in both (*a*) HA–DVS- and (*b*) GMHA-coated samples. Adherent cells on the coated surface surrounding the niches in both (*a*) HA–DVS- and (*b*) GMHA-coated samples stain positive for collagen I, as well as (*c*), (*d*) cells located far from the niches. Nuclei are stained with DAPI (blue) while collagen type-I is stained in red. Scale bar is 100 μm.

samples, 20 kPa and 0.4 kPa, respectively), rather than migrate and populate the microstructures characterized by the same surface coating. Conversely, cells on softer substrates (GEL-SH substrates, 0.2 kPa) neither proliferate on flat nor migrate toward the coated niches. This is in general agreement with studies dealing with cell migration in which cell locomotion occurs faster as the stiffness of the substrate increases (Trichet *et al* 2012). Indeed, in uncoated samples, in which the stiffness of the culture substrate is several orders of magnitude greater than the physiological range, we observed a massive spontaneous colonization of microstructures (Raimondi *et al* 2013, 2014). In contrast to what shown in literature, where gela-tin and other collagen-derived substrates have been proven to enhance cell adhesion and proliferation with respect to culture plastic (Angele *et al* 2004, 2009), we observed a lower cell density both on flat surfaces and in the niches in all coated samples with respect to the uncoated ones. Specifically, the lowest cell density value measured in GEL-SH samples might be due to the slight hydrophobicity of the GEL-SH coating (see the online supporting information (stacks.iop.org/BMM/10/015012)), which might limit cell adhesion proliferation and functions (Kay *et al* 2002, Fan *et al* 2006). Moreover, poor mechanical properties of the GEL-SH coating ($E \sim 0.2$ kPa) may lead to cell detachment due to both hydrogels swelling forces and/or cell traction forces exerted by adherent cells.

The lower cell density measured might explain differences in specific metabolic activity, especially the higher MTT/DNA ratio calculated in in GEL-SH-coated samples. Indeed, a low cell number throughout the GEL-SH samples affects cell migration, crawling and proliferation.

Our preliminary experimental outcomes suggest that the interactions between cells and the microarchitecture allow cells to proliferate and probably maintain the pluripotency because of the 3D adhesive configuration that cells assume in the internal niche volume, even in the presence of a coating material. The effect of the stiffness of the substrate affects cell behavior in terms of morphology, proliferation, migration and colonization of the niches. Cells, interacting with substrates having a lower, more physiological stiffness compared to glass, preferentially adhere on flat coated surfaces instead of migrating and colonizing niches. This is more evident as the rigidity of the substrate decreases. In general, the substrate stiffness seems not to affect the overall cell behavior for cells anchored in the internal niche volume. Conversely, the coating surface with its mechanical properties seems to influence cell migration and differentiation primarily on flat surfaces. Actually, cells on flat coated surface show a greater positivity to collagen I (e.g. in HA–DVS-samples) or at least comparable (e.g. in GMHA-coated samples) to the one estimated on uncoated glass cultured surfaces. Conversely, cells on GEL-SH-coated flat substrates show a significantly

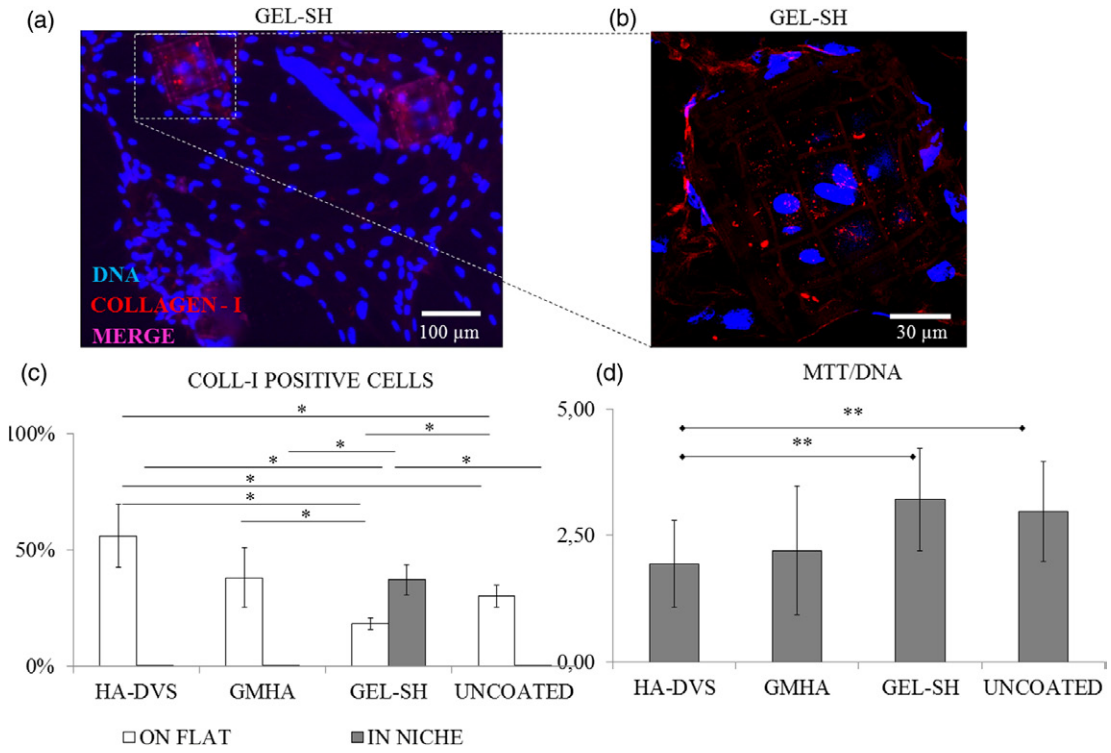

Figure 10. MSC cells cultured on the coated niche substrate at 14 d. (*a*) Fluorescence merged picture and (*b*) Z-stack merged projections of confocal images acquired on GEL-SH-coated niche substrates. Cells within the niche and cells adhering on the external niche walls stain positive for collagen type-I (red), an early marker for osteo-chondral lineage commitment. Cell nuclei are stained with DAPI (blue) and collagen I is stained in red. (*c*) Diagrams for collagen I positive cells normalized with respect to the cell number counted on the coated and uncoated substrates and grouped according to cell location on the substrate ($N = 3$ measurements, $^*p < 0.01$). (*d*) Metabolic activity specific to cells measured for the various hydrogel-coated niche substrates and uncoated controls ($N = 4$ measurements, $^*p < 0.01$).

weaker collagen I expression with respect to all the other coated samples, as well as, on uncoated flat surfaces. This difference might be explained by the physiological range of stiffness of the coating materials that anchored cells sense and react to. Differently, the adhesive configuration in a 3D-like environment (e.g. in the niches), seems to be a relatively stronger cue, in comparison to the coating material stiffness.

To give more conclusive evidences on the effects of the substrate stiffness and the microstructure geometry, an increase of the surface covered by the coated synthetic niches is needed. This improvement will allow us to obtain a critical number of cells to perform quantitative analysis on cell functions (e.g. clonogenic assays, multilineage differentiation assays, PCR analysis for specific genes involved in stem cell fate determination). A further improvement will consist in seeding directly on the coated synthetic niches non-expanded bone marrow cells. Actually, recovering MSCs from bone marrow by their tendency to adhere tightly to plastic culture dishes has been demonstrated to affect cell function. In particular, cells expanded in standard plastic dishes for different culture time, once detached and seeded on PEG substrates having a phototunable stiffness (from relatively rigid to soft) show distinct function. Indeed cells are influenced by their culture history, thus by the sum of all physical cues with which they have interacted (Yang *et al* 2014).

Here we aimed to demonstrate from the technological side, the feasibility of the coating process on such high-resolution microstructures, and the preliminary possibility of decoupling the effects of two mechanical cues that may be involved in guiding stem cell fate differentiation *in vitro*.

5. Conclusion

We have demonstrated an effective methodology to control the surface stiffness of 2PP-engineered micro-scaffolds for stem cell culture. We found that the presence of a coating significantly influences the cell behavior and commitment mainly on the flat surfaces surrounding the niches. Work is in progress to disentangle the roles of the different cues (geometrical and biophysical) in determining the cell behavior in the coated niches. This first study introduces a new and powerful platform to investigate the synergic effects of the 3D microarchitecture and of tailored surface mechanical properties on stem cell fate.

Conflict of interests

The authors have no conflicts of interest to disclose.

Acknowledgments

This project is funded by the Cariplo Foundation (Milano), under grant 2010 '3D Micro-structuring and Functionalisation of Polymeric Materials for Scaffolds in Regenerative Medicine'. We thank Dr Marina Figliuzzi and Dr Irene Catteneo of M. Negri Institue for Pharmacological Research for providing expert help in the immunofluorescence studies.

References

Angele P *et al* 2004 Influence of different collagen species on physico-chemical properties of crosslinked collagen matrices *Biomaterials* **25** 2831–41

Angele P *et al* 2009 Characterization of esterified hyaluronan-gelatin polymer composites suitable for chondrogenic differentiation of mesenchymal stem cells *J. Biomed. Mater. Res. A* **91** 416–27

Anseth K S, Bowman C N and Brannon-Peppas L 1996 Mechanical properties of hydrogels and their experimental determination *Biomaterials* **17** 1647–57

Balazs E A and Leshchiner A 1986 Biomatrix, Inc., assignee. Crosslinked-gels of hyaluronic acid and products containing such gels. Patent No 4,582,865, United States of America

Baier Leach J, Bivens K A, Patrick C W Jr and Schmidt C E 2003 Photocrosslinked hyaluronic acid hydrogels: natural, biodegradable tissue engineering scaffolds *Biotechnol. Bioeng.* **82** 578–89

Bencherif S A, Srinivasan A, Horkay F, Hollinger J O, Matyjaszewski K and Washburn N R 2008 Influence of the degree of methacrylation on hyaluronic acid hydrogels properties *Biomaterials* **29** 1739–49

Bian L, Murat G, Mauck R L and Burdick J A 2013 Hydrogels that mimic developmentally relevant matrix and N-Cadherin interactions enhance MSC chondrogenesis *Proc. Natl Acad. Sci. USA* **110** 10117–22

Collins M N and Birkinshaw C 2011 Morphology of crosslinked hyaluronic acid porous hydrogels *J. Appl. Polym. Sci.* **120** 1040–9

Credi C, Biella S, De Marco C, Levi M, Suriano R and Turri S 2014 Fine tuning and measurement of mechanical properties of crosslinked hyaluronic acid hydrogels as biomimetic scaffold coating in regenerative medicine *J. Mech. Behavior Biomed. Mater.* **29** 309–16

Danilevičius P *et al* 2013 Laser 3D micro/nanofabrication of polymers for tissue engineering applications *Opt. Laser Technol.* **45** 518–24

Engler A J, Sen S, Sweeney HL and Discher DE 2006 Matrix elasticity directs stem cell lineage specification *Cell* **126** 677–89

Fan H, Hu Y, Zhang C, Li X, Lv R, Qin L and Zhu R 2006 Cartilage regeneration using mesenchymal stem cells and a PLGA gelatin/chondroitin/hyaluronate hybrid scaffold *Biomaterials* **27** 4573–80

Flory P J 1953 *Principles of Polymer Chemistry* (Ithaca, NY: Cornell University Press) Retrieved from (http://books.google.es/books?id=CQ0EbEkT5R0C)

Hachet E, Van Den Berghe H, Bayma E, Block MR and Auzély-Velty R 2012 Design of biomimetic cell-interactive substrates using hyaluronic acid hydrogels with tunable mechanical properties *Biomacromolecules* **13** 1818–27

Joddar B and Ito Y 2013 Artificial niche substrates for embryonic and induced pluripotent stem cell cultures *J. Biotechnol.* **68** 218–28

Kay S, Thapa A, Haberstroh K and Webster T 2002 Nanostructured polymer/nanophase ceramic composites enhance osteoblast and chondrocyte adhesion *Tissue Eng.* **8** 753–61

Iyer K, Pulford S, Mogilner A and Shivashankar G 2012 Mechanical activation of cells induces chromatin remodeling preceding MKL nuclear transport *Biophys. J.* **103** 1416–28

Lee H, Dellatore S M, Miller W M and Messersmith P B 2007 Mussel-inspired surface chemistry for multifunctional coatings *Science (New York, NY)* **318** 426–30

Lee H, Rho J and Messersmith PB 2009 Facile conjugation of biomolecules onto surfaces via mussel adhesive protein inspired coatings *Adv. Mater.* **21** 431–4

Marsano E, Gagliardi S, Ghioni F and Bianchi E 2000 Behaviour of gels based on (hydroxypropyl) cellulose methacrylate *Polymer* **41** 7691–8

Maruo S and Fourkas J T 2008 Recent progress in multiphoton microfabrication *Laser Photon. Rev.* **2** 100–111

Mathe G A, Albersdorfer A, Neumaier K R and Sackmann E 1999 Disjoining pressure and swelling dynamics of thin adsorbed polymer films under controlled hydration conditions *Langmuir* **15** 8726–35

Nava M M, Raimondi M T and Pietrabissa R 2012 Controlling self-renewal and differentiation of stem cells via mechanical cues *J. Biomed. Biotechnol.* **2012** 797410

Ovsianikov A, Mironov V, Stampfl J and Liska R 2012 Engineering 3D cell-culture matrices: multiphoton processing technologies for biological and tissue engineering applications *Expert Rev. Med. Devices* **9** 613–33

Pautke C, Schieker M, Tischer T, Kolk A, Neth P, Mutschler W and Milz S 2004 Characterization of osteosarcoma cell lines MG-63, Saos-2 and U-2 OS in comparison to human osteoblasts *Anticancer Res.* **24** 3743–8

Prata J E, Barth T A, Bencherif S A and Washburn N R 2010 Complex fluids based on methacrylated hyaluronic acid *Biomacromolecules* **11** 769–75

Raimondi M T, Eaton S M, Nava M M, Laganà M, Cerullo G and Osellame R 2012 Two-photon laser polymerization: from fundamentals to biomedical application in tissue engineering and regenerative medicine *J. Appl. Biomater. Funct. Mater.* **10** 55–65

Raimondi M T, Eaton S M, Laganà M, Aprile V, Nava M M, Cerullo G and Osellame R 2013 3D structural niches engineered via two-photon laser polymerization promote stem cell homing *Acta Biomater.* **9** 4579–84

Raimondi M T, Nava M M, Eaton S M, Bernasconi A, Vishnubhatla K C, Cerullo G and Osellame R 2014 Optimization of femtosecond laser polymerized structural niches to control mesenchymal stromal cell fate in culture *Micromachines* **5** 341–58

Shu XZ, Ahmad S, Liu Y and Prestwich G D 2006 Synthesis and evaluation of injectable, *in situ* crosslinkable synthetic extracellular matrices for tissue engineering *J. Biomed. Mater. A* **79** 902–12

Shu X Z, Liu Y, Palumbo F and Prestwich G D 2003 Disulfide-crosslinked hyaluronan-gelatin hydrogel films: a covalent mimic of the extracellular matrix for *in vitro* cell growth *Biomaterials* **24** 3825–34

Suh K Y, Yang J M, Khademhosseini A, Berry D, Tran TN, Park H and Langer R 2005 Characterization of chemisorbed hyaluronic acid directly immobilized on solid substrates *J. Biomed. Mater. Res.* B **72** 292–8

Treloar 1975 *The Physics of Rubber Elasticity* (Oxford: Oxford University Press)

Trichet L, Le Digabel J, Hawkins R D, Vedula S R K, Gupta M, Ribrault C, Hersen P, Voituriez R and Ladoux B 2012 Evidence of a large-scale mechanosensing mechanism for cellular adaptation to substrate stiffness *Proc. Natl Acad. Sci.* **109** 6933–8

Vanderhooft J L, Mataz A, Jules J M and Prestwich G D 2009 Rheological properties of cross-linked hyaluronan–gelatin hydrogels for tissue engineering *Macromol. Biosci.* **9** 20–8

Waite J H and Tanzer M L 1981 Polyphenolic substance of mytilus edulis: novel adhesive containing L-dopa and hydroxyproline *Science* **212** 1038–40

Yang C Tibbitt M W, Basta L and Anseth K S 2014 Mechanical memory and dosing influence stem cell fate *Nat. Mater.* **13** 645–52